Epitope Screening Using Hydrogen/Deuterium Exchange Mass Spectrometry (HDX-MS): An Optimized Workflow for Accelerated Evaluation of Lead Monoclonal Antibodies

Shaolong Zhu[1], Peter Liuni[2], Tricia Chen[1], Camille Houy[1], Derek Wilson[2], and Andrew James[1]

[1]Sanofi Pasteur Ltd
[2]York University

July 27, 2021

Abstract

Background: Epitope mapping is an increasingly important aspect of biotherapeutic and vaccine development. Recent advances in therapeutic antibody design and production has enabled candidate mAbs to be identified at a rapidly increasing rate resulting in a significant bottleneck in the characterization of 'structural' epitopes, that are challenging to determine using existing high throughput epitope mapping tools. Here, Hydrogen/Deuterium Exchange Mass Spectrometry (HDX-MS) epitope screening workflow was introduced that is well suited for accelerated characterization of epitopes with a common antigen. Main methods and major results: The method is demonstrated on set of 6 candidate mAbs targeting Pertactin (PRN). Using this approach, five of the six epitopes was unambiguously determined using two HDX mixing timepoints in 24 hours total run time, corresponding to substantial decrease in the instrument time required to map a single epitope using conventional HDX workflows. Conclusion: An accelerated HDX-MS epitope screening workflow was developed. The two-timepoint 'screening' workflow mapped all six mAbs and generated high confidence epitopes for five of the six mAbs assayed. The substantial improvement in the rate of data collection can advance HDX-MS for higher throughput investigations supporting the ability to evaluate a broader number of mAb candidates at an earlier stage of vaccine development.

Shaolong Zhu[1], Peter Liuni[2], Tricia Chen[1], Camille Houy[1], Derek J. Wilson[2], D. Andrew James[1,2*]

[1]Analytical Sciences, Sanofi Pasteur Ltd, Toronto, Ontario, M2R 3T4, Canada

[2]Centre for Research in Mass Spectrometry, Department of Chemistry, York University, Toronto, Ontario, M3J 1P3, Canada

Keywords: Hydrogen/Deuterium Exchange Mass Spectrometry (HDX-MS), epitope screening, monoclonal antibody, Pertactin, vaccine

Corresponding Author

* D. Andrew James, PhD

Sanofi Pasteur Limited

1755 Steeles Ave. W., Toronto M2R 3T4, Canada

Telephone: +1-416-667-2100

Email: Andrew.James@sanofi.com

Abbreviation: HDX-MS, Hydrogen Deuterium Exchange – Mass Spectrometry; mAb, monoclonal antibody; PRN, Pertactin.

Abstract

Background: Epitope mapping is an increasingly important aspect of biotherapeutic and vaccine development. Recent advances in therapeutic antibody design and production has enabled candidate mAbs to be identified at a rapidly increasing rate resulting in a significant bottleneck in the characterization of 'structural' epitopes, that are challenging to determine using existing high throughput epitope mapping tools. Here, Hydrogen/Deuterium Exchange Mass Spectrometry (HDX-MS) epitope screening workflow was introduced that is well suited for accelerated characterization of epitopes with a common antigen.

Main methods and major results: The method is demonstrated on set of 6 candidate mAbs targeting Pertactin (PRN). Using this approach, five of the six epitopes was unambiguously determined using two HDX mixing timepoints in 24 hours total run time, corresponding to substantial decrease in the instrument time required to map a single epitope using conventional HDX workflows.

Conclusion: An accelerated HDX-MS epitope screening workflow was developed. The two-timepoint 'screening' workflow mapped all six mAbs and generated high confidence epitopes for five of the six mAbs assayed. The substantial improvement in the rate of data collection can advance HDX-MS for higher throughput investigations supporting the ability to evaluate a broader number of mAb candidates at an earlier stage of vaccine development.

Introduction

The use of antibody-based therapeutics and reagents has seen unprecedented growth in recent years, with market projections estimated at a combined $212 billion USD annually by 2022.[1] Developments in rapid isolation and enrichment of monoclonal antibodies (mAbs) from challenged serum has simplified the identification of broadly neutralizing and immunogenic antibodies, resulting in a glut of new therapeutic (or vaccine relevant) mAb candiates.[2,3] For vaccines in particular, mAbs selection, with desirable binding attributes, is essential for rational design of *in vitro* potency assays. The challenging aspect now lies in epitope mapping, where the antibody-antigen complex is characterized by the interacting amino acids on the antigen. These amino acids may correspond to a continuous primary sequence (linear epitope) or a 'surface' that is non-contiguous in the primary sequence and results from the 3D structure of the antigen (conformational epitope).[4] Methodologies that can identify both the epitope and binding mechanism are not only desirable but necessary, as pharmaceutical companies must now identify and disclose their epitopes in regulatory filings.[5] Furthermore, pinpointing structurally where the mAb binds to the antigen can provide a direct link to the functional biology associated with neutralization, allowing for an evidence-based conclusion to identify the most valuable mAbs for lead selection.[6],[7]

Currently there are a number of available techniques that can detect epitopes either with high throughput or high resolution. Frequently, more than one method is implemented to confirm identification.[8–10] Synthetic peptide arrays, which use segments of the antigen sequence to bind a mAb target, have made remarkable strides towards high-throughput, whole-proteome, peptide binding assays. Phage display can be used in a similar manner to display whole libraries of peptides on micro-arrays.[11] Neither of these technologies are ideal to identify conformational epitopes and provide little direct information on the binding mechanism. Although, often a time consuming and costly technique, co-crystallization of the mAb-antigen complex followed by X-ray crystallography provides the highest resolution snapshot of an antibody/antigen binding surface and is widely accepted as the 'gold standard' method for epitope/paratope mapping. Residues within 4 angstroms are considered as contacts, but no information on the bond strength of contributing residues or conformational dynamics can be obtained without screening a panel of point mutants.[12] Cryo-electron microscopy is becoming a widely adopted alternative to X-ray crystallography due to its increasingly comparable resolution to X-ray diffraction while offering an inherent increase in throughput.[13] Despite

2

steadily improving high-resolution techniques, it is still desirable that these methods be complimented by approaches that can assess both the structural and dynamic aspects of protein complexes and epitopes in solution. Nuclear magnetic resonance (NMR) spectroscopy is in principle capable of providing dynamic information through a combination of classical structural and relaxation experiments, however this technique requires isotopically labeled material and larger protein complexes (>100 KDa) are difficult to analyse.[14,15]

Hydrogen/Deuterium Exchange Mass Spectrometry (HDX-MS) is an alternative that can characterize both the structural and dynamic aspects of antibody-antigen complexes in-solution.[16–23] It also provides a moderate increase in throughput, while substantially reducing the requirements for purified biological material. Apart from the structural aspect, HDX-MS has also been used to report binding affinities for protein-protein interactions, highlighting the versatility of HDX technology.[24] However, conventional HDX-MS epitope mapping workflows are typically exceedingly lengthy, requiring up to 24 hours of experiment time to generate a single putative epitope. In the current work, we report several refinements to the conventional HDX-MS workflow that substantially increase throughput, while maintaining a high degree of accuracy and precision with epitope assignments using a set of six antibodies targeting pertactin.

Experimental Section

HDX-MS

The HDX experiments were performed as previously described with few modifications.[16,25] For antigen-only HDX experiments, 15 μM of PRN was used and for the complex, equimolar of 15 μM of PRN and mAb were incubated in buffer E (10 mM potassium phosphate buffer pH 7.5). 7.5 μL of the sample was mixed with 32.5 μL of deuterated buffer, buffer L (10 mM potassium phosphate pD 7.5) at 25°C. In the mapping workflow, HDX was conducted at 5 mixing timepoints: 20 sec, 2 min, 10 min, 60 min, and 240 min whereas in the screening workflow, 2 mixing timepoints: 10 min and 30 min were used. All the mapping experiments were conducted in triplicates whereas the screening experiments were performed in duplicates. Mixing in this ratio will attain maximum deuteration of ˜80%. 40 μL of the reaction was quenched in 40 μL of chilled quenching buffer QH (100 mM potassium phosphate, 7.5M GdnHCl, 0.5M TCEP, pH 2.5, 0°C). The quenched samples were then mixed with 80 μL of 0.1% formic acid with subsequent injection of 100 μL of the sample into the nanoACQUITY UPLC HDX module containing protease column for digestion, along with a Waters BEH C18 guard column and ACQUITY CSH C18 analytical column for desalting and separation respectively. The samples were allowed to digest/desalt for 3 min in 0.1% formic acid at a flow rate of 100 μL/min with subsequent separation in the analytical column at a flow rate of 40 μL/min using a 7 min gradient starting from 1% to 60% of water/acetonitrile in 0.1% formic acid. The eluted peptides are detected using Waters Synapt G2-Si mass spectrometer (MA, USA) with acquisition of mass/charge (m/z) range between 300-1700 GluFib (785.8426 m/z) was used as a lock mass solution to maintain mass calibration of <10 ppm. Blank injections (0.1% FA in LC-MS water) were incorporated in between HDX runs to prevent potential carry-over from previous runs.

Peptide identification and HDX analysis

Non-deuterated (0 sec time control) digested peptides were identified by mass accuracy and MS/MS fragmentation (Waters HDMSe function) with the use of software, ProteinLynx Global Server (Waters Corp., MA, USA). Digestion was carried out as same manner as the HDX runs except non-deuterated buffer was used. Fragmentation (HDMSe) was activated in the transfer cell by ramping up the collision energy from 15-65 V.

The quantitative analysis of the HDX data was carried out as previously described with a few modifications.[26,27] The differences for identical peptides between the two states at all the HDX timepoints were calculated and summed. A positive or negative value indicates a decrease or increase in deuterium uptake upon complexation respectively whereas a neutral value indicates no difference. For the mapping workflow, if the differences of absolute sum of the 5 HDX timepoints differences exceeds 1.1 Da and surpass 3 times the standard deviation (σ), then it is considered statistically significant.[27] For screening workflow, if the differences of the summed HDX timepoints exceed 0.5 Da and surpass 3σ, then it is considered signif-

icant as well. σ is defined as the propagated standard deviation of the replicates at mixing timepoints for both states (PRN and PRN/mAb complex). The HDX processing parameters and raw data is attached as supplementary information adhering to the HDX community standards.[28]

The assigned epitopes were mapped onto a three-dimensional structural model generated through homology modelling (Phyre2) using a pre-existing crystal structure, PDB code 1DAB, as a template.[29] Homology model was used as the existing crystal structure lacked the C-terminal linker region. A structural comparison is shown in Figure S1.

Biolayer Interferometry (BLI) peptide/mAb binding experiments.

PRN linear epitope validation experiments were conducted using Biolayer Interferometry (BLI) on a ForteBio Octet RED384 system. All experiments were conducted using ForteBio kinetics buffer (10x kinetic buffer diluted down to 1x using DPBS). Overlapping peptides spanning the predicted epitope site of the mAb were synthesized and biotinylated at its NH_2 terminal (Thermo Fisher Scientific). Furthermore, 2 additional N-terminal biotinylated peptides were synthesized for testing each mAb as negative controls, one that was 100 amino acids upstream and one 100 amino acids downstream from the predicted epitope binding site. The peptides (20 µg/mL) were captured on streptavidin coated biosensors. Sensograms were recorded when peptide-loaded biosensors were incubated with the mAb (20 µg/mL in ForteBio kinetics buffer) and allowed to associate.

Results and discussion

Protease digestion column selection.

Prior to the HDX experiments, a reference peptide library must be generated. This is achieved by subjecting the antigen to proteolysis in the acid-protease digestion column. To maximize relevant information for HDX experiments, the digestion method has to be optimized for sequence coverage and sequence overlap.[30] Digest-peptides should be $5 - 10$ amino acids in length with sequence redundancy, where overlapping peptides can improve the spatial resolution of the data and increase confidence in the measurements.[30] There are several commercially available acid protease options including: pepsin, protease type XIII from *Aspergiluus saitoi,* protease type XVIII from*Rhizhopus* and nepenthesin from *Nepenthes* genus of carnivorous plants among others.[31–33] The digestion efficiency of each protease is dependent on the amino acid properties. For example, pepsin preferentially cleaves bulky hydrophobic residues whereas protease XIII tends to hydrolyze peptide bond with basic amino acids on the C-terminal side.[34,35]For this study, pepsin and protease XIII/pepsin columns were evaluated for digestion efficiency on the model protein pertactin (PRN).

Sequence coverage resulting from protease XIII/pepsin digestion and pepsin digestion are shown in Figure S2. Peptides generated by pepsin cleavage resulted in higher sequence coverage (˜88% of high-quality peptides on average) compared to protease XIII/pepsin column (˜64% on average). While, the protease XIII/pepsin column resulted in slightly higher number overlapping peptides as shown by higher redundancy (2.57 versus 2.25), it also left several gaps in the coverage map. The missing sequences resulting from both protease columns were mapped onto three-dimensional structure is shown in Figure S2. The higher sequence coverage from pepsin can be explained by prevalence of hydrophobic residues in PRN.[36] Pepsin was chosen for the subsequent HDX experiments since it resulted in higher sequence coverage with sufficient sequence redundancy compared to protease XIII/pepsin. Note that fully optimized protease and digestion protocols in epitope mapping are antigen specific, however, there are approaches that will work well for a wide range of antigens and so complete optimization is not always necessary.

Epitope Mapping Workflow.

Six mAbs were evaluated for 'mapping' and 'screening' workflows: mAb 3-4, 3-16, 3-3, 3-21, 3-5, and 1-16. In the 'mapping' workflow, five HDX mixing timepoints, and three replicates, were collected for each antibody. To identify potential binding sites, HDX uptake differences between two states (free PRN versus PRN/mAb complex) were required to exceed the criteria described in the materials and methods section (i.e., difference > 1.1 Da and 3σ).

Differential analysis of the free antigen and the PRN/mAb 1-16 complex revealed one peptide, residues 557-568 surpassing the significance threshold (˜1.4 Da difference) as shown in Figure 1. The representative kinetic plot of peptide 557-568 is provided in Figure S3. The two partially overlapping peptides (555-561) and (558-578) also exhibited decreases in deuterium uptake upon complex formation, though they did not pass the significance threshold (˜0.3 Da and ˜0.3 Da respectively) making residues 562-568 the representative epitope as shown in the heatmap (Figure S4). The heatmap analysis is performed by averaging the relative deuterium uptake of the overlapping peptides, hence providing better resolution of the epitope at the peptide level. This determination provides an example of how overlapping sequences can further resolve the HDX at shorter peptic fragments and potentially to individual amides. The results indicate that the epitope is linear, which was also confirmed using Biolayer Interferometry (BLI) binding studies, where representative peptides containing the linear epitope sequence were evaluated with mAb 1-16. An association curve was generated confirming the binding of the peptide containing the epitope with mAb 1-16 (Figure S5). The assigned epitope was mapped onto the three-dimensional structure of PRN, as shown in Figure 1. This C-terminal region is known to play a critical role in the secretion of PRN through the bacterial membrane as well as providing a template for proper folding of the beta-helix structure of pertactin.[37]

Analysis of the PRN/mAb 3-3 complex also revealed a binding site at the C-terminus. Two peptides (575-591 and 579-591) localized on the C-terminal linker region exhibited the most protection from deuterium update (˜5 Da on average) as shown in Figure 1. The representative kinetic plot of peptide 575-591 is shown in Figure S3. The adjacent peptides, 575-587 and 579-587, however, displayed minimal changes (below 0.25 Da) enabling identification of 588-591 as the epitope. This epitope was also confirmed by BLI binding studies as shown in Figure S6. Interestingly, four other peptides across the sequence exhibited a significant increase in deuterium uptake upon complexation, including residues 35-46, 194-212, 231-245, and 304-313. Although it is unclear why this mAb induced such structural changes, allosteric effects upon antibody/antigen complexation are not a rare phenomenon.[38]

For the PRN/mAb 3-5 complex, only one peptide, 234-244, presented an observable decrease in deuterium uptake during antigen complexation that passed the significance criteria (˜1.5 Da) as shown in Figure 1. The representative kinetic plot of peptide 234-244 is provided in Figure S3. The rest of the protein exhibited negligible differences. A BLI binding study was conducted on mAb 3-5 and peptide 234-244. However, no binding was observed. When PRN was heat denatured at 70°C for various incubation times, there was also reduction in binding as function of time, shown in Figure S7. This result suggest that the epitope is conformational where only one of the binding sites (peptide 234-244) was detectable by HDX (since a linear epitope would not be affected by heat denaturation). Upon analyzing the missing sequences on the 3D structure shown in Figure S2, the loop coverage close to peptide 234-244 was missing. Most likely, this loop was also involved in the binding, but was excluded due to non-detection in the protein digest. Peptide 234-244 is part of the polymorphic region of PRN (residues ˜230-260) where variation has been linked to immune evasion.[39,40] Hence binding to this region may impact immune escape functionality.

Three mAbs described thus far bind to PRN on continuous sections of the sequence, mainly comprised of loops or disordered regions localized on the surface of the protein, as shown in Figure 1. These results align with other studies where epitopes were most commonly found to be in surface exposed, less-structured regions of antigens.[41,42] Binding to linear, continuous epitope does not depend on the tertiary fold of the antigen but is linked only to the binding sequence.[4,43] Hence antibodies binding to a linear epitope can be tested using a denatured antigen or an unstructured peptide containing the epitope sequence.[4,43] Conformational epitopes, however, are dependent on the fold of the antigen. As such, binding is highly sensitive to the correct tertiary structure of the antigen, corresponding to at least one configuration of the 'native' conformational ensemble.[4,43] It has been estimated that ˜90% of the antibodies recognize conformational epitopes.[44]

Differential analysis of the PRN/mAb 3-16 complex detected two peptides, 36-46 and 56-67, in the N-terminus with deuterium uptake differences of 4.5 Da and ˜3 Da respectively (Figure 1). Structurally, these two peptides are in close proximity to one another, indicating characteristics of a conformational epitope. The kinetic plots for these two peptides are provided in Figure S3. All other peptides across the sequence

5

showed negligible differences except for increase in deuterium uptake in peptide 231-245 which is part of the polymorphic regions of PRN responsible for immune evasion, similar to mAb 3-3.[39,40] The N-terminus is immunogenic and some of the known immunogenic epitopes in the N-terminus are known to be masked by the polymorphic region.[45,46] Increased flexibility of the polymorphic region could indicate "unmasking" of the epitope in the N-terminus for efficient binding of mAb 3-16.[46]

In the PRN/mAb 3-21 complex, five peptides from the N-terminal region, 35-46, 47-54, 55-67, 68-78 and 109-116, exhibited decreases in deuterium that surpassed the significance criteria suggesting a conformational epitope (Figure 1). This epitope included the sequences detected for mAb 3-16 (peptides 36-46 and 56-67) which suggests that these two mAbs share a common epitope. However, when an epitope binning experiment (i.e., a competitive binding assay) was performed using biolayer interferometry, both mAbs were able to bind to PRN simultaneously, suggesting different epitope location. The remaining sequences: 47-54, 68-78 and 109-116 were then mapped onto the protein structure. Residues 47-54 and 109-116 are in close proximity whereas 68-78 is localized on the opposite face of the antigen, same side as residues 36-46 and 56-67, as shown in Figure S8. Hence a tentative assignment for a conformational epitope corresponding to peptides 47-54 and 109-116 was made. The kinetic plots for two representative peptides, 47-54 and 108-116 are shown in Figure S3.

Finally, epitope mapping analysis of PRN/mAb 3-4 revealed a decrease in deuterium uptake localized on the C-terminal end of PRN specifically peptides 420-436, 455-464, 477-492, and 505-517 as shown in Figure 1. The kinetic plots for these four peptides are shown in Figure S3. These sites are all in close proximity to each other, with a majority of residues in loop regions. It is plausible that some of these residues took up less deuterium due to steric hindrance effects, since a large surface area was impacted.[47] Nevertheless, the data indicates that this is a conformational epitope. This epitope is localized near another PRN polymorphic variation region (residues 545-566).[39,40] This PRN polymorphic region contains tandemly repeated sequences (Pro-Gln-Pro-) that have been implicated in immune evasion by either insertion or deletion of repeat units. Hence mAb binding to this epitope may directly impact the immune escape functionality of PRN by affecting the flexibility of the polymorphic region such that hidden epitopes downstream of C-terminus are unmasked.[46] Similar to the linear epitopes, all the identified conformational epitopes were localized on surface-exposed loops and/or sheet-loop structures.[42,47]

Screening workflow.

In developing the screening workflow, two HDX timepoints (10 min or 30 min) were acquired. Single time-points were also assessed for feasibility of epitope detection. HDX results for individual timepoints are shown in Figure S9. For all mAbs, results from the 30 min timepoint were more ambiguous than for the 10 min timepoint, as demonstrated by weaker or no deuterium-uptake signals. For example, PRN/mAb 1-16 and PRN/mAb 3-5 complexes did not show clear epitope detection at 30 minutes labeling time, although one peptide in the mAb 1-16 epitope (575-587) and one in the mAb 3-5 epitope (234-244) showed the highest uptake difference (qualitatively) while surpassing the 3σ. Nonetheless, these uptake differences were comparable to those observed in other peptides across the antigen sequence. In the PRN/mAb3-3 complex, there were two peptides, 229-236 and 579-591, that exhibited HDX differences at 30 minutes of labelling. However, these two peptides were spatially distant and defining an epitope against the protein structure was difficult. Analysis of 10 minutes HDX timepoint showed clear HDX differences allowing for slightly improved epitope assignment. However, the results were often only marginally substantial and in some cases were indistinguishable from differences occurring across the sequence (i.e., 'noise' in HDX difference data). Ultimately, the HDX differences for both timepoints (10 and 30 min) were summed in the screening workflow, which amplified non-random differences to the minimum extent required to enable confident epitope assignments, as shown in Figure 2. As with the 'mapping' workflow, a significant change was defined as uptake differences exceeding 0.5 Da in both HDX timepoints and surpassing 3σ from at least two technical replicates.

The HDX differences observed using the in the screening workflow were lower than those acquired from the full time-course, mapping workflow (an unsurprising consequence of adding together fewer timepoint measurements). These changes can be seen in deuterium uptake (y-axis) of the Difference plots comparing

6

mapping results in Figure 1 to screening results in Figure 2. The primary benefit to the screening approach is that it provides substantial enhancements to throughput; all six mAb/PRN complexes were screened in the same amount of time required to 'map' a single antibody/antigen interaction using the full time-course workflow. The acquisition and analysis for all states of PRN complexed with the different mAbs, was performed simultaneously in one dataset, as opposed to data collection in separate experiment/days. Thus, this type of analysis can also more easily identify artifact peptides/signals. However, the caveat for simultaneous analysis is that it requires consistent, high quality peptide signals for all the PRN states. Even if a subset of states shows poor peptide signal response, that peptide must be excluded from analysis, which may impact sequence coverage, or sequence redundancy. Nonetheless in the screening dataset presented here, the sequence coverage is ~88%, which is identical to the 'mapping' workflow. The summary of epitopes identified from the 'screening' workflow is shown in Table S1.

Analysis of the PRN/mAb 3-4 complex found residues 427-436, 455-464, and 477-492 exhibiting the greatest uptake differences (Figure 2). This represents a substantial overlap with regions identified in the mapping workflow (Figure 1), however; the screening data lacked sequence coverage between 504 and 541, preventing a direct comparison in the $505 - 517$ region, which was assigned to the epitope in the mapping workflow. For the PRN/mAb 3-16 complex, regions of 35-46 and 56-67 exhibited the most difference (Figure 2), perfectly superimposing the differences from the mapping workflow (Figure 1). PRN/mAb 3-5 also exhibited the greatest HDX difference in the 237-244 region (Figure 2), in alignment with the epitope identified in the mapping workflow (region 234-244, Figure 1). In the PRN/mAb 3-3 complex, only one peptide near the C-terminus, 579-591, showed a significant difference, which was also consistent with the mapping workflow (Figure 1 and Figure 2). The PRN/mAb 1-16 complex did not exhibit a large difference in uptake upon complexation in either workflow, which made the data interpretation challenging. Nevertheless, one peptide, 558-574, surpassed the 3σ significance criterion in the screening data (Figure 2). While too large to provide good localization of an epitope, this sequence still contains the segment identified in the mapping workflow (562-568, Figure 1). For the PRN/mAb 3-21complex, the screening experiment identified residues 35-67 and 108-117 as the most affected regions (Figure 2), while peptide 68-78 showed negligible difference (refer to Figure S8 for peptide 68-78 localization on the structure). While not identical, this is similar to the mapping workflow, which identified segments $47 - 54$ and 109-116 to be the epitope (Figure 1).

Overall, the epitopes identified through the screening workflow were in good agreement with the mapping workflow for both conformational and linear epitopes. The mapping workflow utilizes many time points across wide range (seconds – hours). The advantage of using such a wide range is that it can improve confidence in the assignments of epitopes, especially for cases where summing differences across multiple timepoints is required to achieve statistical certainty based on strict significance criteria. Furthermore, the kinetics data acquired in the mapping workflow can also provide additional information on the kinetics of the protein complex dissociation relative to the rate of the deuterium uptake.[48] The screening workflow, on the other hand, takes two snapshots, which offers at best highly limited rate information. However, when the aim is specifically to determine the epitope and not to characterize the antibody/antigen interaction in detail, the screening workflow balances confidence in the epitope assignment with substantially improved throughput.

Concluding remarks

In this work, we developed an accelerated workflow for epitope mapping using hydrogen deuterium exchange mass spectrometry and demonstrated it using six mAbs targeting the pertussis antigen PRN. The classical five timepoint 'mapping' workflow required 144 hours of instrument time to map all six epitopes and generated high confidence epitopes for five of the six mAbs assayed. The two-timepoint 'screening' workflow required 24 hours of instrument time to map all six mAbs and generated high confidence epitopes for five of the six mAbs assayed. The remaining epitope was correctly identified, but not fully mapped (mAb 3-5) in both workflows. The high degree of correlation between these two methods suggests that, at least for the strict purpose of identifying epitopes, acquiring more than two time points may be of little value. Given the increasingly rapid rate at which new therapeutic and test mAbs are being generated, we are confident this approach, which

allows a seven-fold improvement in the rate of data collection, will be an attractive alternative, opening the door to medium throughput epitope screening by HDX-MS.

The accelerated workflow introduced here will provide a means to advance HDX-MS for higher throughput investigations in vaccine and drug development, supporting the ability to evaluate a broader number of mAb candidates at an earlier stage of development.

CONFLICTS OF INTEREST

Shaolong Zhu (SZ) and Peter Liuni (PL) were industrial postdoctoral fellows when experiments in this study were performed. Camille Houy (CH) was part of the Volunteer for International Experience (VIE) program at Sanofi Pasteur Lmt Canada at the time this study was performed. SZ and CH are now employees of Eurofins PSS. PL is now an employee of Sciex. Tricia Chen and D. Andrew James are employees of Sanofi Pasteur Lmt Canada. Derek J. Wilson declares no competing interests.

REFERENCES

[1] Carter, P. J., Lazar, G. A., Next generation antibody drugs: pursuit of the 'high-hanging fruit'. *Nature Reviews Drug Discovery* **2017** , 17:197–223.

[2] Wine, Y., Boutz, D. R., Lavinder, J. J., Miklos, A. E., Hughes, R. A., Hoi, K. H., Jung, S. T., Horton, A. P., Murrin, E. M., Ellington, A. D., Marcotte, E. M., Georgiou, G., Molecular deconvolution of the monoclonal antibodies that comprise the polyclonal serum response.*PNAS* **2013** , 110:2993–2998.

[3] Corti, D., Langedijk, J. P. M., Hinz, A., Seaman, M. S., Vanzetta, F., Fernandez-Rodriguez, B. M., Silacci, C., Pinna, D., Jarrossay, D., Balla-Jhagjhoorsingh, S., Willems, B., Zekveld, M. J., Dreja, H., O'Sullivan, E., Pade, C., Orkin, C., Jeffs, S. A., Montefiori, D. C., Davis, D., Weissenhorn, W., McKnight, Á., Heeney, J. L., Sallusto, F., Sattentau, Q. J., Weiss, R. A., Lanzavecchia, A., Analysis of Memory B Cell Responses and Isolation of Novel Monoclonal Antibodies with Neutralizing Breadth from HIV-1-Infected Individuals.*PLOS ONE* **2010** , 5:e8805.

[4] Van Regenmortel, M. H. V., What is a B-cell epitope?*Methods Mol. Biol.* **2009** , 524:3–20.

[5] Davidson, E., Doranz, B. J., A high-throughput shotgun mutagenesis approach to mapping B-cell antibody epitopes.*Immunology* **2014** , 143:13–20.

[6] Howell, K. A., Qiu, X., Brannan, J. M., Bryan, C., Davidson, E., Holtsberg, F. W., Wec, A. Z., Shulenin, S., Biggins, J. E., Douglas, R., Enterlein, S. G., Turner, H. L., Pallesen, J., Murin, C. D., He, S., Kroeker, A., Vu, H., Herbert, A. S., Fusco, M. L., Nyakatura, E. K., Lai, J. R., Keck, Z.-Y., Foung, S. K. H., Saphire, E. O., Zeitlin, L., Ward, A. B., Chandran, K., Doranz, B. J., Kobinger, G. P., Dye, J. M., Aman, M. J., Antibody Treatment of Ebola and Sudan Virus Infection via a Uniquely Exposed Epitope within the Glycoprotein Receptor-Binding Site.*Cell Rep* **2016** , 15:1514–1526.

[7] Saphire, E. O., Schendel, S. L., Fusco, M. L., Gangavarapu, K., Gunn, B. M., Wec, A. Z., Halfmann, P. J., Brannan, J. M., Herbert, A. S., Qiu, X., Wagh, K., He, S., Giorgi, E. E., Theiler, J., Pommert, K. B. J., Krause, T. B., Turner, H. L., Murin, C. D., Pallesen, J., Davidson, E., Ahmed, R., Aman, M. J., Bukreyev, A., Burton, D. R., Crowe, J. E., Davis, C. W., Georgiou, G., Krammer, F., Kyratsous, C. A., Lai, J. R., Nykiforuk, C., Pauly, M. H., Rijal, P., Takada, A., Townsend, A. R., Volchkov, V., Walker, L. M., Wang, C.-I., Zeitlin, L., Doranz, B. J., Ward, A. B., Korber, B., Kobinger, G. P., Andersen, K. G., Kawaoka, Y., Alter, G., Chandran, K., Dye, J. M., Systematic Analysis of Monoclonal Antibodies against Ebola Virus GP Defines Features that Contribute to Protection. *Cell* **2018** , 174:938-952.e13.

[8] Abbott, W. M., Damschroder, M. M., Lowe, D. C., Current approaches to fine mapping of antigen–antibody interactions.*Immunology* **2014** , 142:526–535.

[9] Buus, S., Rockberg, J., Forsström, B., Nilsson, P., Uhlen, M., Schafer-Nielsen, C., High-resolution Mapping of Linear Antibody Epitopes Using Ultrahigh-density Peptide Microarrays. *Mol Cell Proteomics***2012** , 11:1790–1800.

[10] Reineke, U., Schutkowski, M., *Epitope mapping protocols***2009** Humana Press, New York.

[11] Rojas, G., Tundidor, Y., Infante, Y. C., High throughput functional epitope mapping: Revisiting phage display platform to scan target antigen surface. *MAbs* **2014** , 6:1368–1376.

[12] Chakraborti, S., Prabakaran, P., Xiao, X., Dimitrov, D. S., The SARS Coronavirus S Glycoprotein Receptor Binding Domain: Fine Mapping and Functional Characterization. *Virology Journal* **2005** , 2:73.

[13] Merk, A., Bartesaghi, A., Banerjee, S., Falconieri, V., Rao, P., Davis, M. I., Pragani, R., Boxer, M. B., Earl, L. A., Milne, J. L. S., Subramaniam, S., Breaking Cryo-EM Resolution Barriers to Facilitate Drug Discovery. *Cell* **2016** , 165:1698–1707.

[14] Blech, M., Peter, D., Fischer, P., Bauer, M. M. T., Hafner, M., Zeeb, M., Nar, H., One target-two different binding modes: structural insights into gevokizumab and canakinumab interactions to interleukin-1β. *J. Mol. Biol.* **2013** , 425:94–111.

[15] Zuiderweg, E. R. P., Mapping Protein-Protein Interactions in Solution by NMR Spectroscopy. *Biochemistry* **2002** , 41:1–7.

[16] Zhu, S., Liuni, P., Ettorre, L., Chen, T., Szeto, J., Carpick, B., James, D. A., Wilson, D. J., Hydrogen–Deuterium Exchange Epitope Mapping Reveals Distinct Neutralizing Mechanisms for Two Monoclonal Antibodies against Diphtheria Toxin. *Biochemistry* **2019** , 58:646–656.

[17] Malito, E., Biancucci, M., Faleri, A., Ferlenghi, I., Scarselli, M., Maruggi, G., Lo Surdo, P., Veggi, D., Liguori, A., Santini, L., Bertoldi, I., Petracca, R., Marchi, S., Romagnoli, G., Cartocci, E., Vercellino, I., Savino, S., Spraggon, G., Norais, N., Pizza, M., Rappuoli, R., Masignani, V., Bottomley, M. J., Structure of the meningococcal vaccine antigen NadA and epitope mapping of a bactericidal antibody. *Proc Natl Acad Sci U S A* **2014** , 111:17128–17133.

[18] Huang, R. Y.-C., Krystek, S. R., Felix, N., Graziano, R. F., Srinivasan, M., Pashine, A., Chen, G., Hydrogen/deuterium exchange mass spectrometry and computational modeling reveal a discontinuous epitope of an antibody/TL1A Interaction. *MAbs* **2018** , 10:95–103.

[19] Bertoldi, I., Faleri, A., Galli, B., Lo Surdo, P., Liguori, A., Norais, N., Santini, L., Masignani, V., Pizza, M., Giuliani, M. M., Exploiting chimeric human antibodies to characterize a protective epitope of Neisseria adhesin A, one of the Bexsero vaccine components.*FASEB J* **2016** , 30:93–101.

[20] Li, J., Wei, H., Krystek, S. R., Bond, D., Brender, T. M., Cohen, D., Feiner, J., Hamacher, N., Harshman, J., Huang, R. Y.-C., Julien, S. H., Lin, Z., Moore, K., Mueller, L., Noriega, C., Sejwal, P., Sheppard, P., Stevens, B., Chen, G., Tymiak, A. A., Gross, M. L., Schneeweis, L. A., Mapping the Energetic Epitope of an Antibody/Interleukin-23 Interaction with Hydrogen/Deuterium Exchange, Fast Photochemical Oxidation of Proteins Mass Spectrometry, and Alanine Shave Mutagenesis. *Anal Chem* **2017** , 89:2250–2258.

[21] Batsuli, G., Deng, W., Healey, J. F., Parker, E. T., Baldwin, W. H., Cox, C., Nguyen, B., Kahle, J., Königs, C., Li, R., Lollar, P., Meeks, S. L., High-affinity, noninhibitory pathogenic C1 domain antibodies are present in patients with hemophilia A and inhibitors.*Blood* **2016** , 128:2055–2067.

[22] Giuliani, M., Bartolini, E., Galli, B., Santini, L., Lo Surdo, P., Buricchi, F., Bruttini, M., Benucci, B., Pacchiani, N., Alleri, L., Donnarumma, D., Pansegrau, W., Peschiera, I., Ferlenghi, I., Cozzi, R., Norais, N., Giuliani, M. M., Maione, D., Pizza, M., Rappuoli, R., Finco, O., Masignani, V., Human protective response

9

induced by meningococcus B vaccine is mediated by the synergy of multiple bactericidal epitopes. *Sci Rep* **2018** , 8:3700.

[23] Sun, H., Ma, L., Wang, L., Xiao, P., Li, H., Zhou, M., Song, D., Research advances in hydrogen–deuterium exchange mass spectrometry for protein epitope mapping. *Anal Bioanal Chem* **2021** , 413:2345–2359.

[24] Zhu, M. M., Rempel, D. L., Du, Z., Gross, M. L., Quantification of protein-ligand interactions by mass spectrometry, titration, and H/D exchange: PLIMSTEX. *J. Am. Chem. Soc.* **2003** , 125:5252–5253.

[25] Wales, T. E., Fadgen, K. E., Gerhardt, G. C., Engen, J. R., High-Speed and High-Resolution UPLC Separation at Zero Degrees Celsius. *Anal. Chem.* **2008** , 80:6815–6820.

[26] Houde, D., Engen, J. R., Conformational analysis of recombinant monoclonal antibodies with hydrogen/deuterium exchange mass spectrometry. *Methods Mol. Biol.* **2013** , 988:269–289.

[27] Houde, D., Berkowitz, S. A., Engen, J. R., The utility of hydrogen/deuterium exchange mass spectrometry in biopharmaceutical comparability studies. *J Pharm Sci* **2011** , 100:2071–2086.

[28] Masson, G. R., Burke, J. E., Ahn, N. G., Anand, G. S., Borchers, C., Brier, S., Bou-Assaf, G. M., Engen, J. R., Englander, S. W., Faber, J., Garlish, R., Griffin, P. R., Gross, M. L., Guttman, M., Hamuro, Y., Heck, A. J. R., Houde, D., Iacob, R. E., Jørgensen, T. J. D., Kaltashov, I. A., Klinman, J. P., Konermann, L., Man, P., Mayne, L., Pascal, B. D., Reichmann, D., Skehel, M., Snijder, J., Strutzenberg, T. S., Underbakke, E. S., Wagner, C., Wales, T. E., Walters, B. T., Weis, D. D., Wilson, D. J., Wintrode, P. L., Zhang, Z., Zheng, J., Schriemer, D. C., Rand, K. D., Recommendations for performing, interpreting and reporting hydrogen deuterium exchange mass spectrometry (HDX-MS) experiments. *Nat Methods* **2019** , 16:595–602.

[29] Kelley, L. A., Mezulis, S., Yates, C. M., Wass, M. N., Sternberg, M. J. E., The Phyre2 web portal for protein modeling, prediction and analysis. *Nat Protoc* **2015** , 10:845–858.

[30] Nirudodhi, S. N., Sperry, J. B., Rouse, J. C., Carroll, J. A., Application of Dual Protease Column for HDX-MS Analysis of Monoclonal Antibodies. *Journal of Pharmaceutical Sciences* **2017** , 106:530–536.

[31] Zhang, Z., Smith, D. L., Determination of amide hydrogen exchange by mass spectrometry: a new tool for protein structure elucidation. *Protein Sci.* **1993** , 2:522–531.

[32] Yang, M., Hoeppner, M., Rey, M., Kadek, A., Man, P., Schriemer, D. C., Recombinant Nepenthesin II for Hydrogen/Deuterium Exchange Mass Spectrometry. *Anal. Chem.* **2015** , 87:6681–6687.

[33] Cravello, L., Lascoux, D., Forest, E., Use of different proteases working in acidic conditions to improve sequence coverage and resolution in hydrogen/deuterium exchange of large proteins. *Rapid Commun. Mass Spectrom.* **2003** , 17:2387–2393.

[34] Zhang, H.-M., Kazazic, S., Schaub, T. M., Tipton, J. D., Emmett, M. R., Marshall, A. G., Enhanced digestion efficiency, peptide ionization efficiency, and sequence resolution for protein hydrogen/deuterium exchange monitored by Fourier transform ion cyclotron resonance mass spectrometry. *Anal. Chem.* **2008** , 80:9034–9041.

[35] Sachdev, G. P., Fruton, J. S., Secondary enzyme-substrate interactions and the specificity of pepsin. *Biochemistry* **1970** , 9:4465–4470.

[36] Emsley, P., Charles, I. G., Fairweather, N. F., Isaacs, N. W., Structure of Bordetella pertussis virulence factor P.69 pertactin. *Nature* **1996** , 381:90–92.

[37] Junker, M., Schuster, C. C., McDonnell, A. V., Sorg, K. A., Finn, M. C., Berger, B., Clark, P. L., Pertactin beta-helix folding mechanism suggests common themes for the secretion and folding of autotransporter proteins. *Proc Natl Acad Sci U S A* **2006** , 103:4918–4923.

[38] Mazza, M. M., Retegui, L. A., Monoclonal antibodies to human growth hormone induce an allosteric conformational change in the antigen. *Immunology* **1989** , 67:148–153.

[39] Gravekamp, C., Rosner, B., Madoff, L. C., Deletion of repeats in the alpha C protein enhances the pathogenicity of group B streptococci in immune mice. *Infect. Immun.* **1998** , 66:4347–4354.

[40] Hijnen, M., Mooi, F. R., van Gageldonk, P. G. M., Hoogerhout, P., King, A. J., Berbers, G. A. M., Epitope structure of the Bordetella pertussis protein P.69 pertactin, a major vaccine component and protective antigen. *Infect. Immun.* **2004** , 72:3716–3723.

[41] Rubinstein, N. D., Mayrose, I., Halperin, D., Yekutieli, D., Gershoni, J. M., Pupko, T., Computational characterization of B-cell epitopes. *Mol. Immunol.* **2008** , 45:3477–3489.

[42] Sollner, J., Grohmann, R., Rapberger, R., Perco, P., Lukas, A., Mayer, B., Analysis and prediction of protective continuous B-cell epitopes on pathogen proteins. *Immunome Res* **2008** , 4:1.

[43] Barlow, D. J., Edwards, M. S., Thornton, J. M., Continuous and discontinuous protein antigenic determinants. *Nature* **1986** , 322:747–748.

[44] Haste Andersen, P., Nielsen, M., Lund, O., Prediction of residues in discontinuous B-cell epitopes using protein 3D structures. *Protein Sci* **2006** , 15:2558–2567.

[45] Inatsuka, C. S., Xu, Q., Vujkovic-Cvijin, I., Wong, S., Stibitz, S., Miller, J. F., Cotter, P. A., Pertactin is required for Bordetella species to resist neutrophil-mediated clearance. *Infect. Immun.* **2010** , 78:2901–2909.

[46] Hijnen, M., de Voer, R., Mooi, F. R., Schepp, R., Moret, E. E., van Gageldonk, P., Smits, G., Berbers, G. A. M., The role of peptide loops of the Bordetella pertussis protein P.69 pertactin in antibody recognition. *Vaccine* **2007** , 25:5902–5914.

[47] Kringelum, J. V., Nielsen, M., Padkjær, S. B., Lund, O., Structural analysis of B-cell epitopes in antibody:protein complexes. *Molecular Immunology* **2013** , 53:24–34.

[48] Zhang, Z., Vachet, R. W., Kinetics of Protein Complex Dissociation Studied by Hydrogen/Deuterium Exchange and Mass Spectrometry. *Anal Chem* **2015** , 87:11777–11783.

FIGURES AND FIGURE LEGENDS

Hosted file

`image1.emf` available at https://authorea.com/users/427855/articles/531927-epitope-screening-using-hydrogen-deuterium-exchange-mass-spectrometry-hdx-ms-an-optimized-workflow-for-accelerated-evaluation-of-lead-monoclonal-antibodies

Figure 1. Epitope mapping difference plot between PRN and PRN/mAb (1-6, 3-3, 3-5, 3-16, 3-21, and 3-4) complexes. Red dashed lines represent the 1.1 Da threshold and the blue dashed lines represent 3σ. The epitopes are highlighted in coloured stars according to the mAbs tested and are also coded in the three-dimensional structure with the corresponding colours.
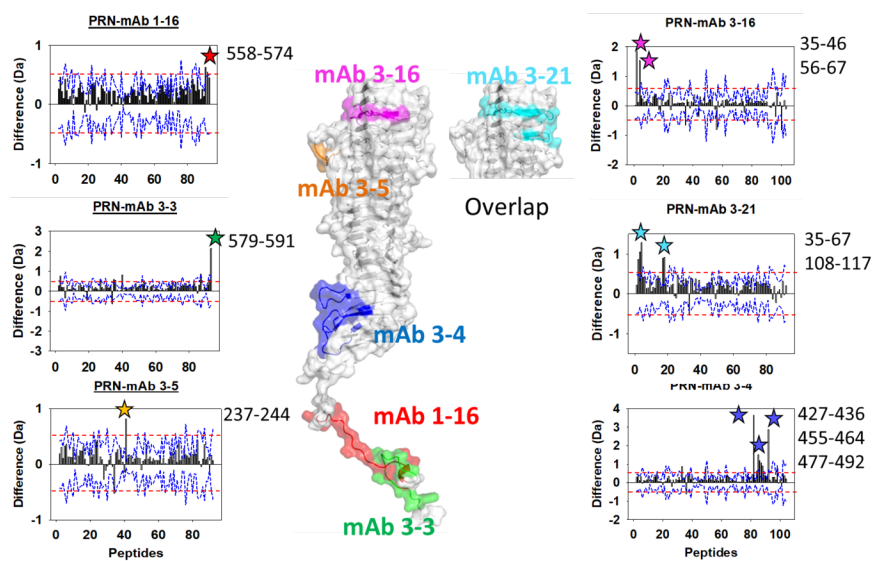
Figure 2. Epitope screening difference plot between PRN and six mAb complexes. The epitopes are highlighted in coloured stars and are highlighted in the three-dimensional structure with the corresponding colours